PHYSICAL REVIEW A **95**, 061402(R) (2017)

X-ray versus Auger emission following Xe 1*s* photoionization

M. N. Piancastelli,[1,2,3,*] K. Jänkälä,[4] L. Journel,[1,3] T. Gejo,[3,5] Y. Kohmura,[3] M. Huttula,[4] M. Simon,[1,3] and M. Oura[3]

[1]*Sorbonne Universités, UPMC Université Paris 06, CNRS, UMR 7614, Laboratoire de Chimie Physique-Matière et Rayonnement, F-75005 Paris, France*

[2]*Department of Physics and Astronomy, Uppsala University, Box 516, SE-75120 Uppsala, Sweden*

[3]*RIKEN SPring-8 Center, 1-1-1 Kouto, Sayo-cho, Sago-gun, Hyogo 679-5148, Japan*

[4]*Nano and Molecular Systems Research Unit, University of Oulu, Box 3000, FI-90014, Oulu, Finland*

[5]*Graduate School of Materials Science, University of Hyogo, Kamigori-cho, Ako-gun 678-1297, Japan*

(Received 15 February 2017; published 13 June 2017)

Xe 1*s* photoelectron spectra were measured at SPring-8, Japan. The core-hole lifetime broadening was found to be 9.6 eV, yielding a lifetime of ∼68 as. The amount of radiative versus nonradiative decay was assessed by recording Auger *LMM* spectra below and above the *K* edge. Below the *K* edge, *L* vacancies are produced only by direct photoionization, while above the *K* edge some of these vacancies are mainly produced by *K L* emission following 1*s* photoionization. Due to the dipole selection rule for x-ray emission, the dominant role of the *K L* relaxation process is rather directly observed.

DOI: 10.1103/PhysRevA.95.061402

I. INTRODUCTION

The investigation of photoemission and decay processes around very deep edges is a field in its infancy. This is due to the requirement of very high-energy photon sources and suitable detection systems. Historically, very high-energy photon sources have been available in nuclear physics, namely, in the fields of β- and γ-ray spectroscopy [1], primarily used to study nuclear levels, nuclear disintegration schemes, β emission, and internal conversion processes. Also, very high-kinetic-energy Auger spectra have been measured by β capture by the nucleus followed by internal conversion [2]. However, the use of such sources in electron spectroscopy has been quite limited, and those have been replaced by the much lower-energy but more versatile x-ray ones used for electron spectroscopy for chemical analysis (ESCA) [3]. As for more modern sources such as synchrotron radiation, although in principle x rays of tens of keV are available at some high-energy facilities, no photoemission studies of isolated atoms and molecules are reported at binding energies of several tens of keV.

The 1*s* ionization potential of a prototypical system, Xe, is reported around 34 565.13 eV [4]. The study of the dynamics of Xe photoionization and the subsequent decay of xenon around the *K* edge can provide fundamental information about the core-hole lifetime of such a deep vacancy, satellite structure, and interplay between radiative and nonradiative decay. However, the published literature on photoexcitation and photoionization of Xe 1*s* is scarce and mainly consists of absorption data complemented with theoretical calculations [4–7], and fluorescence measurements [8–11]. High-energy Auger electrons (*KLL*, *KLM*, *KMM*) have also been measured following β capture and internal conversion [12]. No recent experimental data on Xe 1*s* photoionization or decay via Auger or x-ray emission are reported.

A direct measurement of the Xe 1*s* photoelectron spectrum and subsequent multistep Auger decay has been hindered up to now by the lack of suitable instrumentation. However, such experiments are nowadays feasible at the storage ring SPring-8, Japan. We have recorded there the Xe 1*s* photoelectron spectrum and the subsequent *LMM* Auger decay, with a total instrumental line broadening much narrower that the core-hole lifetime width. To the best of our knowledge, this is the highest-binding-energy photoelectron line measured. The Xe 1*s* spectrum shows a very broad main peak, followed by a rather complex satellite structure. Due to the very large core-hole lifetime broadening, giving rise to a spectral structure with a full width half maximum (FWHM) of 13.4 eV, the satellite structure is unresolved, but we have been able to assign it on the ground of relativistic Dirac-Fock calculations. By a careful fitting of the experimental spectrum with a Voigt function which takes into account all possible experimental broadenings, we can give the value of 9.6 ± 0.2 eV as the core-hole lifetime broadening, corresponding to a lifetime of 68 ± 2 attoseconds (as).

To complement the 1*s* photoelectron spectra, we have measured and calculated the *LMM* Auger spectra. The main point is that *LMM* Auger decay can provide one crucial piece of information, namely, the relative amount of radiative versus nonradiative decay. The rationale is the following: Just below the Xe *K* edge, direct photoionization of the *L* edge is possible, with subsequent *LMM* Auger decay. Above the *K* edge, after Xe 1*s* photoionization, the system has two main decay pathways: *KLL* Auger, followed by Auger cascade, or *K L* x-ray emission, in turn followed by another Auger cascade. The Xe *L*-edge single vacancies can therefore be produced by two different avenues, namely, either by direct photoionization or after *K L* x-ray emission. However, the dipole selection rule governing the *K L* decay prevents it from reaching 2*s* vacancies, and only 2*p* vacancies can be created this way.

We have measured and calculated the Xe *LMM* Auger spectra below and above the *K* edge. We have found substantial differences between the two spectra, mainly due to the dipole selection rule for radiative decay. The consequence of such

*maria-novella.piancastelli@physics.uu.se

a selection rule is the following: Above threshold, where the major decay process is KL, only $2p$ vacancies can be populated, and therefore the *LMM* Auger spectra bear the signature of such selectivity. Namely, the $L_{2,3}MM$ decay above threshold is clearly dominant over the L_1MM one, which is negligible on a relative scale, at variance with the below-threshold spectra.

The present *ab initio* method gives a calculated KL radiative decay versus *KLL* nonradiative decay a fluorescence yield of $90.1 \pm 1\%$, and a *total* K-shell fluorescence yield of $89.0 \pm 1\%$, consistent with the value $88.9 \pm 1\%$ already estimated in the literature [10]. Even though the present measurement does not allow one to directly determine the value of radiative/Auger decay ratio, a good agreement between the experimental and calculated *LMM* spectra clearly indicates that the ratio is really in the region of 90%. This finding provides experimental evidence of the dominance of radiative versus nonradiative decay for heavy systems.

II. EXPERIMENT

Measurements were carried out at the experimental hutch 3 of the BL29XU undulator beamline [13]. The photon energy range of the beamline reaches 40 keV. A monochromatic photon beam in the 32.0–35.6 keV energy range was obtained using a Si(111) double-crystal monochromator cooled by liquid nitrogen [14]. The energy resolution of the photon beam, i.e., $\Delta E/E$, was about 1.66×10^{-4}. The photon beam was collimated to a size of $0.5 \times 0.5\,\mathrm{mm}^2$ using a four-jaw slit before introducing it into an apparatus. In order to measure the electron spectra, the apparatus equipped with a hemispherical electron energy analyzer (Scienta Omicron [15] SES-2002 and a gas-cell GC-50) was used. During the measurement, the target gas pressure was maintained to be about 5×10^{-3} Pa outside the gas cell. The lens axis of the analyzer was in the horizontal direction at right angles to the photon beam direction and parallel to the polarization vector of the incoming photons. The apparatus was mounted on a position-adjustable XZ stage. The energy scale of the incident photon beam was calibrated by measuring the K-absorption spectrum of Zr foil and also by recording the $1s$ photoelectron spectra of Ar and Kr atoms [16]. The energy scales of the electron spectra were calibrated by measuring the Auger electron spectra and the photoelectron spectra of Ar and Kr atoms. Well-established Ar *KLL* and *KLM* lines [17] and a Xe LMM^1G line [18] were used as references. In the measurements, the energy resolution of the analyzer was set to be 3.9 eV. The photon band pass was theoretically calculated to be 5.9 eV at 35.6 keV. The thermal Doppler broadening is around a few meV and is negligible. Thus the overall resolution for the measurements can be estimated to be 7.1 eV.

III. THEORY

Theoretical calculations were carried out in a relativistic configuration interaction Dirac-Fock framework, where the total atomic state functions are constructed as linear combinations of the same total angular momentum J and parity P. The basis of the linear combinations were jj-coupled configuration state functions (CSFs), formed as determinantal products of one-electron orbitals. The coefficients of the linear combination were solved by diagonalizing the Dirac-Coulomb-Breit Hamiltonian in the CSF basis with fixed radial one-electron functions. The one-electron wave functions were obtained in the average level scheme by applying the GRASP2K package [19] with a modified Rscf component from the GRASP92 program [20]. The atomic state function (ASF) mixing coefficients and further relativistic and QED corrections were solved using the Relci extension [21] of GRASP. The corrections included transverse Breit interactions, mass shifts, contributions from self-energy, and vacuum polarization as implemented in Relci [21]. The inclusion of the corrections is critical since, for example, the largest corrections (Breit and self-energy) yield about a 120 eV shift to the calculated K-shell binding energy of Xe [22].

All calculations included only such orbitals that are occupied in the ground state of Xe. The ground state, K and L singly ionized states, and $1s^{-1}5p^{-1}nl$ satellite states were calculated within the single configuration scheme. The final states of the presented *LMX* Auger spectrum included all states obtainable from *MM*, *MN*, and *MO* double-hole configurations. For obtaining correct lifetime broadenings of the L ionized states, Auger decays to all doubly ionized states *MX*, *NX*, and *OO*, where $X = M,N,O$ were performed. In addition, because the considered double core-hole states can decay further, Auger decays to all possible triply ionic states *MMM*, *MNN*, *MNO*, and *NNN* were calculated. The total lifetime broadening of the presented *LMX* Auger electron lines are thus defined by the sum of the broadenings of initial L hole state and final *MX* double hole state. The partial (*KL*) and total (*KX*) fluorescence yields were calculated by dividing the radiative decay rates with their respective sums of radiative and nonradiative decay rates (*KLL* and *KXX′*). The used computational method does not provide a systematic way to estimate errors for the calculated fluorescence yields, but based on the sensitivity of the values to a change of gauge from length to velocity in fluorescence matrix elements and small variations, such as exclusion of the exchange interaction in the generation of continuum waves in Auger decay, we give a rough estimate of $\pm 1\%$.

The Auger and fluorescence decay transition-matrix elements were calculated utilizing the Auger and Reos components of the RATIP package [21,23], respectively. The relative intensities of the photoionization monopole satellites were calculated within the sudden approximation where the probability is defined by the orbital overlap integrals between the ground and ionized states (see, e.g., Ref. [24]). All fluorescence decay and photoionization matrix elements were calculated in the length gauge.

IV. RESULTS AND DISCUSSION

The Xe $1s$ experimental and calculated photoelectron spectra are shown in Fig. 1. The calibrated incident photon energy was $35\,542 \pm 6$ eV. The kinetic energy scale is calibrated by spectral features appearing between 600 and 450 eV kinetic energy (not shown), which stem from Auger *MNN* decay and have a well-known energy position [25]. The Xe $1s$ binding energy derived from our measurements is therefore 34 565 eV, in good agreement with the literature value of 34 565.13 eV [4].

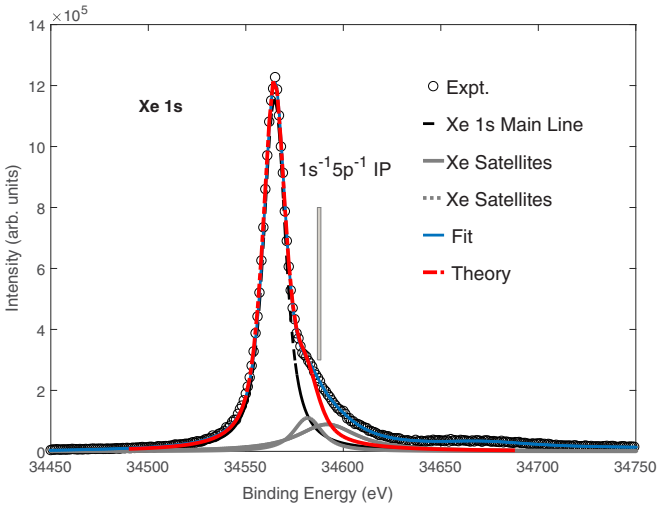

FIG. 1. Experimental and theoretical Xe 1s photoelectron spectra. Fit results are also shown. The calculated double-ionization threshold $1s^{-1}5p^{-1}$ is also marked.

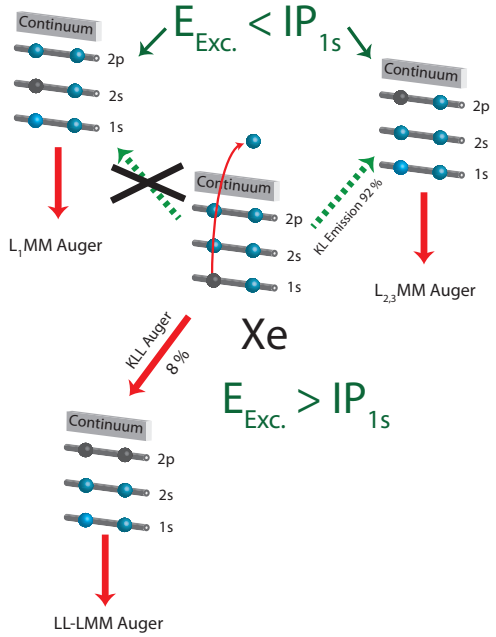

FIG. 2. Schematic view of the relaxation processes taking place below and above the Xe 1s ionization threshold. The main decay pathways are marked by green arrows (x-ray emission) and red arrows (Auger emission).

This value is confirmed by our calculations, which give a theoretical value of 34 563.6 eV.

The experimental peak has 13.4 eV full width half maximum (FWHM), and shows a long tail due to a satellite structure extending by almost 50 eV from the main line. By our calculations, we are able to assign the main satellite contributions (see Table I) and the $1s^{-1}5p^{-1}$ double-ionization threshold (indicated in the figure).

The slight discrepancy in intensity between experimental and theoretical curves in the higher-energy satellite region is due to the missing contributions from conjugate shakeups and double excitations whose calculation is beyond the focus of the present Rapid Communication.

The 1s photoelectron peak has been fitted by using four Voigt functions with the same Gaussian width, taking into account the experimental resolution (∼7 eV). The relative energy positions of the most intense satellite structures with respect to the main line have been set and derived from the Xe 2s photoelectron spectrum (not shown). By taking into account the instrumental broadening factors such as the photon bandwidth (5.9 eV) and the electron analyzer resolution (3.9 eV), we are able to give the core-hole lifetime broadening Γ as 9.6 ± 0.2 eV, corresponding by the standard formula $\Gamma = \hbar/\tau$ to a lifetime τ of 68 ± 2 as. In the literature the value 11.4 eV is reported for the Xe 1s linewidth [26,27], derived mainly from fluorescence data or from estimated and/or adapted values. However, no discussion is reported there either on the relative importance of instrumental broadening or of the interplay of the lifetimes of the initial and final state of the KL emission in determining the linewidth of the fluorescence. We believe that with our method we can obtain a more precise determination of the lifetime of such a deep core hole.

In Fig. 2 we show a pictorial illustration of the main decay processes following Xe L-edge and K-edge ionization, and their possible interplay. It is clearly shown that LMM Auger decay can take place after vacancies in the L shell are created either by direct photoemission or by KL x-ray emission. It is also shown that while $2p$ holes can be created both ways, $2s$ holes cannot be reached by KL emission, due to the dipole selection rule, but only by direct photoionization. Therefore it is possible to take advantage of this selection

TABLE I. Assignment and energy ranges of main satellite contributions. Left: Energy ranges as the distance from the top of the Xe 1s main line. Right: Energy ranges in binding energy calculated at the calibrated photon energy of 35 542 eV.

	Energy ranges of satellite spectra			
	Distance from threshold (eV)		Binding energy (eV)	
	Lowest value	Highest value	Lowest value	Highest value
$5p \rightarrow 5d$	12.9	18.9	34572.5	34578.5
$5p \rightarrow 6s$	13.1	15.0	34572.7	34574.6
$5p \rightarrow 6p$	15.0	17.3	34574.6	34576.9
$5p \rightarrow 7p$	18.4	20.4	34578.0	34580.0
$5p \rightarrow 8p$	19.8	21.7	34579.4	34581.3
$5p \rightarrow$ continuum	22.1	23.9	34581.7	34583.5

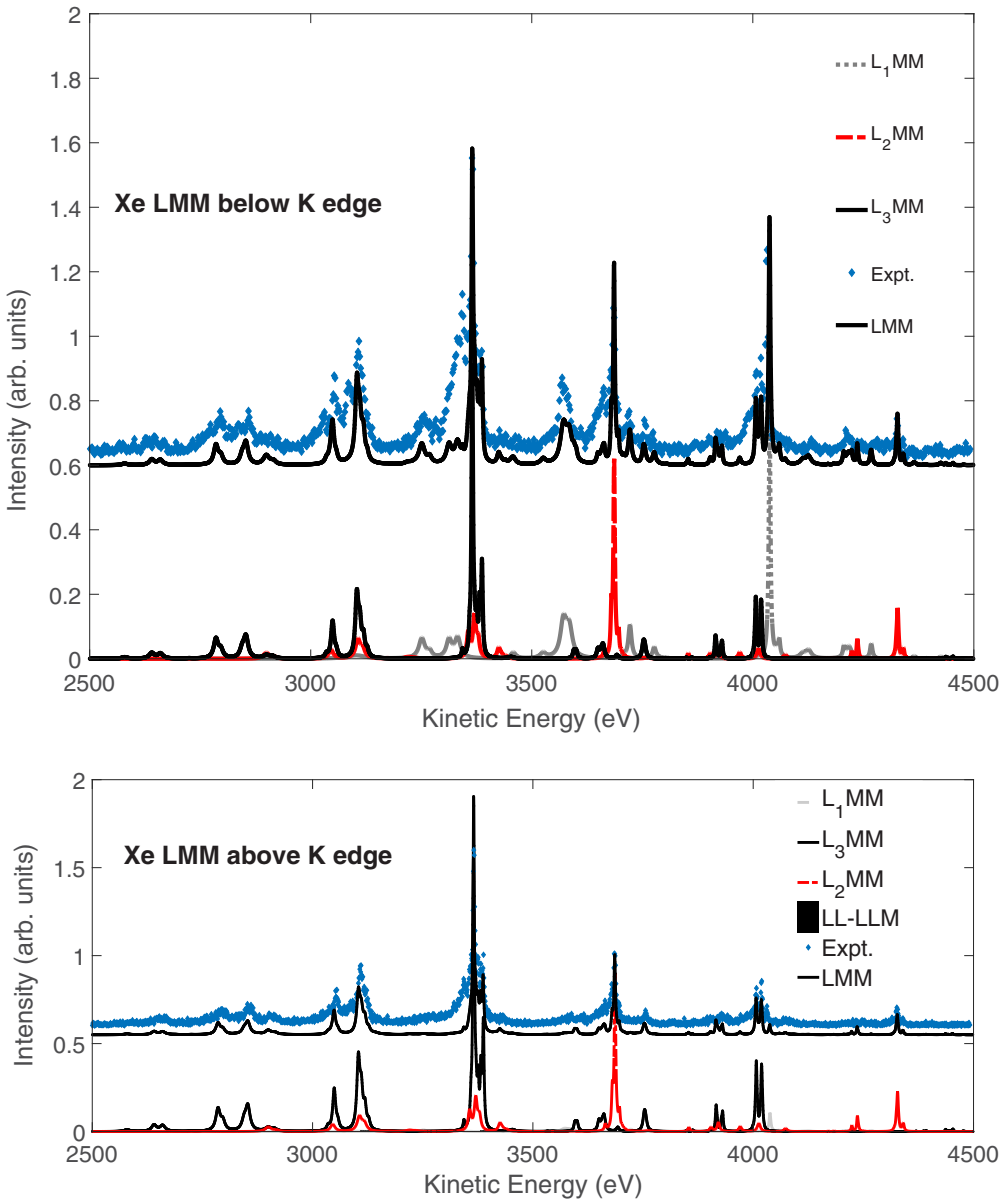

FIG. 3. Experimental and calculated Xe *LMM* Auger spectra below (top) and above (bottom) the Xe 1*s* photoionization threshold. The photon energies are 31 951 eV for the top spectrum and 35 443 eV for the bottom one. The composition of the calculated spectra to show their main contributions is reported in the lower part of each figure, while the total calculated spectra compared with the experimental ones are shown in the upper part.

rule to estimate the importance of radiative decay (see a more detailed discussion below).

In Fig. 3 we show the *LMM* Auger spectra recorded below (top) and above (bottom) the 1*s* ionization threshold. The two photon energies are 31 951 and 35 443 eV, respectively. The breakdown of the theoretical spectra into components arising from L_1MM, $L_{2,3}MM$, and LL-LMM (above threshold) Auger decay is reported in the lower part of the figures, while in the upper part the total theoretical spectrum is shown and compared with the experimental spectrum. A very good agreement is evident between experimental and theoretical spectra. A more detailed assignment of all structures obtained by the calculations is outside the scope of the present work and will be reported in a forthcoming publication [28].

We can clearly see that the Auger peaks related to the decay of the L_1 edge are greatly reduced in relative intensity by comparing both experimental and theoretical spectra below and above threshold. The explanation is the following. Below threshold, the *LMM* Auger spectrum originates from the decay following direct ionization of the L edge, while above threshold there can be several contributions: direct ionization of the L shell, second-step Auger decay after *KLL*, and finally, and most importantly, Auger decay of $L_{2,3}$ edges reached after KL emission (see Fig. 2).

The greatly reduced relative intensity of the L_1MM Auger decay above threshold is due to the dipole selection rule governing the KL decay pattern: By x-ray emission $2p_{3/2}$ and $2p_{1/2}$ singly charged final states can be reached, but not

states with a 2s hole. Therefore the basic disappearance of spectral structures due to L_1MM Auger emission is a clear consequence of the KL x-ray emission being the dominant decay channel after 1s photoionization. The observed behavior is supported by calculations done for photoionization cross sections. In the investigated photon energy region the L-shell photoionization cross sections do not change rapidly. In fact, they decrease by about 40% between the two selected photon energies separated by about 3500 eV. It can be also seen in the calculations that, at the selected energy above the K-shell threshold, the 1s photoionization cross section is about ten times larger than the 2s cross section, 37 times larger than the $2p_{1/2}$ cross section, and 25 times larger than the $2p_{3/2}$ cross section. This indicates that most of the intensity of the observed *LMM* Auger spectrum above the K-shell threshold is due to 1s ionization followed by $KL_{2,3}$ fluorescence emission.

Another important result from the calculations is the following: If the relaxation process of the 1s vacancy proceeds via Auger emission, the first step is *KLL*, creating two vacancies in the L shell, followed by an Auger cascade of the type *LL-LMM*, and then *LMM-MMMM*. In the kinetic energy region of the Auger *LMM* emission, some of the states reached after *LL-LMM* relaxation should be included. However, there is no evidence for such spectral features in the experimental spectrum. The calculations reveal that the intensity of *LL-LMM* second-step Auger decay is negligible. The corresponding calculated spectrum is reported in the lower part of Fig. 3 (bottom), and shows very clearly that such a decay pattern is very weak. This is another evidence of the Auger decay being a minority channel after the creation of a 1s hole.

V. CONCLUSION

In conclusion, we have analyzed the Xe 1s photoelectron spectrum with state-of-the-art experimental and theoretical methods. We have assigned the related complex satellite structure, and derived the core-hole lifetime. Furthermore, from a detailed analysis of the *LMM* Auger decay, we show that the great majority of decay processes after Xe 1s photoionization imply the emission of photons (radiative decay) rather than electrons (nonradiative decay). The percentage of radiative decay is determined as $89.0 \pm 1\%$, given by the calculated total decay rates between radiative and nonradiative relaxation channels. Although the dominance of radiative decay is a well-known phenomenon from a theoretical standpoint, our method provides a rather direct way to observe it.

These results will open the way for investigations of molecules containing heavy atoms with comparable core binding energies, as, e.g., iodine. Some of us have recently shown that ultrafast dissociation is possible to observe in the Auger cascade following the creation of a core hole (Cl 1s) with lifetime of 1 fs [29], and to follow the related wave-packet dynamics [30]. Nuclear dynamics started by core-hole lifetimes in the attosecond range will then become possible to observe.

ACKNOWLEDGMENTS

The experiment was performed at BL29XU of SPring-8 with the approval of RIKEN (Proposal No. 20160025). The authors are grateful to the member of the engineering team of the RIKEN SPring-8 Center for their technical assistance.

[1] *Beta- and Gamma-Ray Spectroscopy*, edited by K. Siegbahn (North-Holland, Amsterdam, 1955), and references therein.

[2] *Alpha-, Beta-, and Gamma-Ray Spectroscopy*, edited by K. Siegbahn (North-Holland, Amsterdam, 1965), and references therein.

[3] K. M. Siegbahn, Nobel Lecture: "Electron Spectroscopy for Atoms, Molecules and Condensed Matter," http://www.nobelprize.org/nobel_prizes/physics/laureates/1981/siegbahn-lecture.html

[4] R. D. Deslattes, E. G. Kessler, Jr., P. Indelicato, L. de Billy, E. Lindroth, and J. Anton, Rev. Mod. Phys **75**, 35 (2003), and references therein.

[5] B. W. Holland, J. B. Pendry, R. F. Pettifer, and J. Bordas, J. Phys. C: Solid State Phys. **11**, 633 (1978).

[6] A. N. Hopersky, V. A. Yavna, and V. A. Popov, J. Phys. B: At. Mol. Opt. Phys. **30**, 5131 (1997).

[7] M. Deutsch, G. Brill, and P. Kizler, Phys. Rev. A **43**, 2591 (1991).

[8] M. Hribar, A. Kodre, and J. Pahor, Z. Phys. A **280**, 227 (1977).

[9] E. G. Kessler, Jr., R. D. Deslattes, D. Girard, W. Schwitz, L. Jacobs, and O. Renner, Phys. Rev. A **26**, 2696 (1982).

[10] J. H. Hubbell, P. N. Trehan, N. Singh, B. Chand, D. Mehta, M. L. Garg, R. R. Garg, S. Singh, and S. Puri, J. Phys. Chem. Ref. Data **23**, 339 (1994), and references therein.

[11] T. Mooney, E. Lindroth, P. Indelicato, E. G. Kessler, Jr., and R. D. Deslattes, Phys. Rev. A **45**, 1531 (1992).

[12] A. Kovalıka, V. M. Gorozhankin, A. F. Novgorodov, M. A. Mahmoud, N. Coursol, E. A. Yakushev, and V. V. Tsupko-Sitnikov, J. Electron Spectrosc. Relat. Phenom. **95**, 231 (1998).

[13] K. Tamasaku, Y. Tanaka, M. Yabashi, H. Yamazaki, N. Kawamura, M. Suzuki, and T. Ishikawa, Nucl. Instrum. Methods A **467-468**, 686 (2001).

[14] T. Mochizuki, Y. Kohmura, A. Awaji, Y. Suzuki, A. Baron, K. Tamasaku, M. Yabashi, H. Yamazaki, and T. Ishikawa, Nucl. Instrum. Methods A **467-468**, 647 (2001).

[15] The analyzer as well as the gas cell were originally supplied by Gammadata Scienta.

[16] M. Breinig, M. H. Chen, G. E. Ice, F. Parente, and B. Crasemann, Phys. Rev. A **22**, 520 (1980).

[17] L. Asplund, P. Kelfve, B. Blomster, H. Siegbahn, and K. Siegbahn, Phys. Scr. **16**, 268 (1977).

[18] G. B. Armen, T. Aberg, J. C. Levin, B. Crasemann, M. H. Chen, G. E. Ice, and G. S. Brown, Phys. Rev. Lett. **54**, 1142 (1985).

[19] P. Jönsson, X. He, C. Froese Fischer, and I. P. Grant, Comput. Phys. Commun. **177**, 597 (2007).

[20] F. A. Parpia, C. Froese Fischer, and I. P. Grant, Comput. Phys. Commun. **94**, 249 (1996).

[21] S. Fritzsche, C. Froese Fischer, and G. Gaigalas, Comput. Phys. Commun. **148**, 103 (2002).

[22] J. Niskanen, K. Jänkälä, M. Huttula, and A. Föhlisch, J. Chem. Phys. **146**, 144312 (2017).
[23] S. Fritzsche, C. Froese Fischer, and C. Z. Dong, Comput. Phys. Commun. **124**, 340 (2000).
[24] T. A. Carlson and C. W. Nestor, Jr., Phys. Rev. A **8**, 2887 (1973).
[25] L. Partanen, M. Huttula, S.-M. Huttula, H. Aksela, and S. Aksela, J. Phys. B: At. Mol. Opt. Phys. **39**, 4515 (2006).
[26] M. O. Krause and J. H. Oliver, J. Phys. Chem. Ref. Data **8**, 329 (1979), and references therein.
[27] J. L. Campbell and T. Papp, At. Data Nucl. Data Tables **77**, 1 (2001).
[28] R. Püttner, K. Jänkälä, M. Simon, M. N. Piancastelli *et al.* (unpublished).
[29] O. Travnikova *et al.*, Phys. Rev. Lett. **116**, 213001 (2016).
[30] O. Travnikova *et al.* (unpublished).